Progress in Organic Coatings 69 (2010) 184–192

Contents lists available at ScienceDirect

Progress in Organic Coatings

journal homepage: www.elsevier.com/locate/porgcoat

Modification of zinc powder to improve the corrosion resistance of weldable primers

A.C. Bastos [a,*], M.L. Zheludkevich [a], I. Klüppel [b], G. Grundmeier [c], M.G.S. Ferreira [a]

[a] DECV/CICECO, Universidade de Aveiro, 3810-193 Aveiro, Portugal
[b] Dortmunder Oberflächencentrum GmbH, Eberhardstraße 12, 44145 Dortmund, Germany
[c] University of Paderborn, Warburger Str. 100, 33098 Paderborn, Germany

ARTICLE INFO

Article history:
Received 24 July 2009
Received in revised form 15 April 2010
Accepted 23 April 2010

Keywords:
Weldable primers
Coil-coatings
EIS
SVET
Corrosion
Zinc powder

ABSTRACT

This paper reports the modification of zinc powder to improve the corrosion resistance of weldable primers. These primers are thin zinc rich organic coatings applied by roll coating at the steel manufacturer. The automotive industry uses them to protect areas in the car body that become inaccessible after joining processes. In this work, with the objective of increasing the corrosion resistance of these systems, the zinc particles were chemically treated or simply replaced by powder of 55AlZn alloy. The rest of the formulation remained intact. The performance of the commercial and modified formulations was compared by SEM, SVET and EIS. The best results were obtained when the zinc powder was replaced by powder of the aluminium zinc alloy.

1. Introduction

A problem faced by the automotive industry is the low corrosion resistance of areas in the car body that cannot be effectively reached by pre-treatments or cathodic electro-paints as, for example, flanged joints, still crevices and cavities created after joining processes. Usually those areas are sealed with waxes and adhesives which bring construction limitations and raise the costs. One way to overcome the problem is to pre-coat the steel with paints that allow the welding of coated metals. The metal substrate can be pre-painted at the steel producer by coil coating, increasing its corrosion resistance, before it becomes inaccessible by the joining processes.

Weldable primers (WPs) were introduced in the automotive industry in Europe in 1995 [1]. These systems consist of electrogalvanised steel (EG) with a chromate-free pre-treatment and a zinc rich epoxy-based coil coating applied on the top of it. The function of the zinc powder is to make the primer weldable by providing the electrical contact between the welding electrode and the metal substrate. The amount of zinc powder present is not enough to provide cathodic protection. Furthermore, the primer is applied to the zinc layer, not directly to steel. The anticorrosive protection is achieved through the barrier effect provided by the primer and can be further enhanced by the use of inhibiting additives. Schnell et al. reported that in a cyclic corrosion test the protection effect of these WPs is 3 times higher in comparison to EG without paint [1]. The corrosion protection would be improved by thicker primers, but thin films are used, typically 2.5–4.5 μm, to reduce the alloying of zinc with the copper welding electrodes, which is the main reason for the decrease of electrodes' life. A new stage of development started in 1999 to double the corrosion resistance of the 1st generation primers, in a joint effort between the automotive industry and the steel, paint and pre-treatment producers [1]. Additionally it was important to reduce the cure temperature from 260 °C to about 150–160 °C in order to use bake-hardening steel grades that are sensitive to higher curing temperatures. It is difficult to increase the corrosion protection without decreasing the welding properties. Two approaches have been followed to develop 2nd generation primers. The first was to keep the zinc powder systems but optimize the binder and use special additives. The second approach was to use iron phosphide, Fe_2P, or mixtures of iron phosphide and zinc powder. Fe_2P has a high melting point and is inert regarding copper electrodes. In any case, the 2nd generation WPs provide better corrosion resistance (6 times that of EG, the double compared to the 1st generation) and the welding properties are very good [1]. The disadvantage of using Fe_2P is that it is very hard and problems were found regarding adhesion, tool wear and tool pollution during forming [2]. Due to these disadvantages only zinc based systems are in use today.

---

[*] Corresponding author at: Dept. Eng. Cerâmica e do Vidro, Universidade de Aveiro, Campus Universitario de Santiago, 3810-193 Aveiro, Portugal.
E-mail address: acbastos@ua.pt (A.C. Bastos).

0300-9440/$ – see front matter © 2010 Elsevier B.V. All rights reserved.
doi:10.1016/j.porgcoat.2010.04.021

Table 1
Weldable primers tested.

	Modification on the formulation	Film thickness (μm)
WP1	Commercial formulation	3.5
WP2	Zinc powder treated with cerium nitrate	3.5
WP3	Zinc powder treated with mercaptobenzothiazole	3.5
WP4	Zinc powder treated with organosilane	3.5
WP5	Zinc powder replaced by 55AlZn powder	3.5
WP6	Zinc powder replaced by 55AlZn powder	6.5

The work now reported follows the first mentioned approach. The idea is to continue using the 1st generation primers with their advantages in terms of formability, adhesion, tool wear and tool pollution, but improving the corrosion resistance. Some organic and inorganic zinc corrosion inhibitors were tested to extend the lifetime of WPs while immersed in aqueous NaCl solutions [3]. The inhibition of zinc powder corrosion in NaCl solutions after a pre-treatment with the same inhibitors was also studied [4].

The present paper concludes this line of work by testing the anticorrosive performance of WPs formulations using modified zinc powder. A commercial WP of 1st generation was used as reference system and the formulation was modified through the incorporation of zinc powder treated by an inorganic corrosion inhibitor (cerium nitrate), an organic corrosion inhibitor (2-mercaptobenzothiazole) and an organosilane adhesion promoter (3-glycidoxypropyltrimethoxysilane). In a parallel set of experiments the zinc powder was replaced by powder of an aluminium zinc alloy, 55AlZn. The corrosion resistance of all coatings was tested in 0.05 M NaCl by the Scanning Vibrating Electrode Technique (SVET), Electrochemical Impedance Spectroscopy (EIS) and Scanning Electron Microscopy (SEM).

2. Experimental procedure

2.1. Powder modification

The treatment of the zinc powder with cerium nitrate was made by stirring 200 g of zinc powder with 200 mL of 10^{-3} M $Ce(NO_3)_3$ during 1 h, then filtered in a glass filter with a water pump and dried at 100 °C for 30 min. To treat with 2-mercaptobenzothiazole (MBT), 200 g of zinc powder were stirred with 300 mL of 0.5 g L^{-1} MBT in 95% water + 5% ethanol during 1 h, washed with ethanol and dried at 50 °C for 1 h. The silane treatment of the zinc powder was made with 3-glycidoxypropyltrimethoxysilane (Glymo): 250 g of zinc powder and 300 mL of Glymo solution (1% Glymo + 16% isopropanol + 83% water) were added to a beaker and stirred for 1 h. The mixture was filtered with jet pump, rinsed 3 times with pure ethanol, dried at room temperature and then at 60 °C during 1 h. Zinc powder was also replaced by 55AlZn powder. The mean particle sizes were 11.2 μm for zinc powder and 7.8 μm for 55AlZn powder. All reagents used in the modification of zinc powder were of *pro analysis* grade.

2.2. Painted systems

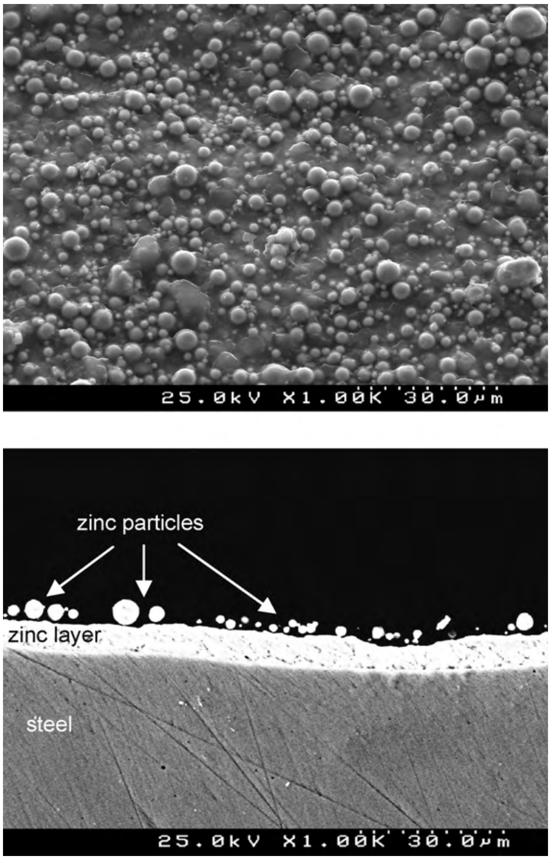

Fig. 1. Surface and cross-section micrographs of WP1 before immersion.

The weldable primers were produced by a paint manufacturer after receiving the modified powders—Table 1. Formulation and manufacture were similar for all coatings. The primers were applied in a laboratory sized roll coater followed by curing in a continuous furnace with a peak metal temperature of 260 °C (furnace temperature ~360 °C). The nominal film thickness was 3.5 μm for all systems, except WP6, which was 6.5 μm. Since the nominal thickness (h) is smaller than the particles' size, the method used for its determination was based in the weight difference of a substrate plate before and after coating (Δm) and applying the following equation:

$$h = \frac{\Delta m}{\rho A} \tag{1}$$

where ρ is the dry film density, given by the paint supplier and A is the area of the plate (typically 20 cm × 10 cm). This is the most accurate method for thickness determination under these circumstances.

The metal substrate was low carbon DC06 steel sheet [5], 0.8 mm thick with an electroplated zinc layer with 7 μm of nominal thickness. A commercial chromate-free pre-treatment was applied before the paint, in the same way as the commercial system. The amount of metallic powder in the dry film of all formulations was 73 ± 1 wt%.

2.3. SVET

SVET measurements were performed on samples of 1 cm × 1 cm that were glued to an epoxy cylinder support. A mixture of beeswax + colophony was used to insulate the sample leaving only a window of a few squared millimeters that was exposed to the testing solution. Adhesive tape was applied around the epoxy support to make a solution reservoir. Measurements were made with Applicable Electronics Inc. (USA) instrumentation and controlled by the ASET software from ScienceWares (USA). The vibrating microelectrodes had a 10 μm spherical platinum black tip and vibrated with amplitude of 10 μm at an average distance of 200 μm from

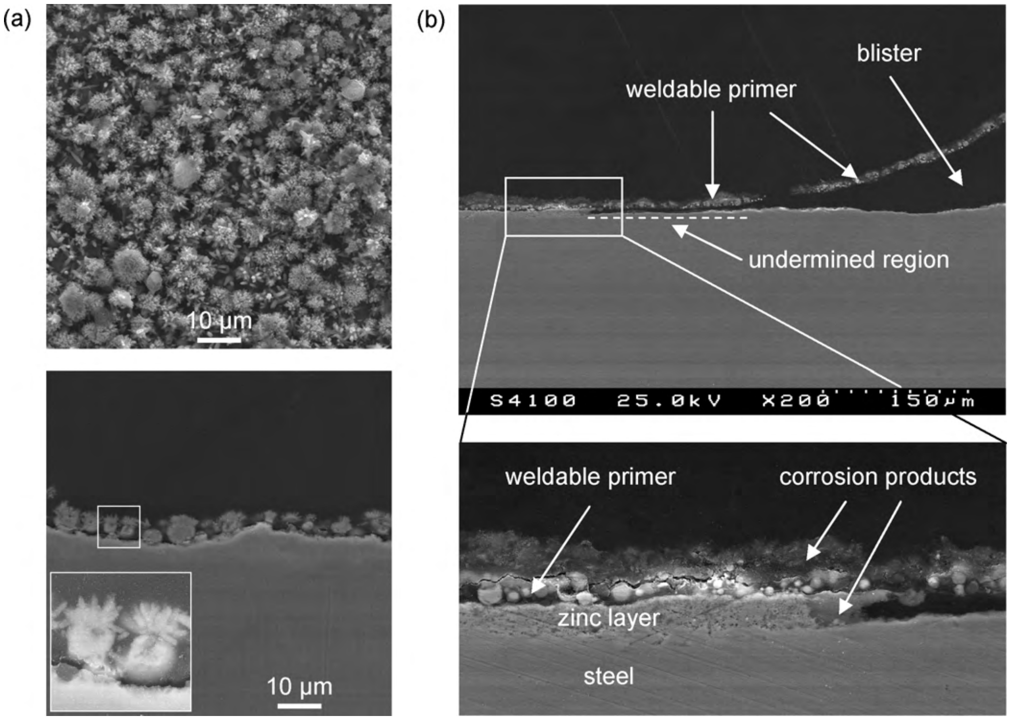

Fig. 2. Micrographs of WP1 after 15 days of immersion in 0.05 M NaCl taken (a) in the region with less corrosion products and (b) in the border of a blister.

the surface of the sample. Each scan comprised 50 × 50 points and a duration of ~1000s (with an acquisition time of 0.3 s in each point).

2.4. EIS

The electrochemical cells for EIS measurements were prepared by gluing polymethylmethacrylate tubes to the surface of the primer with epoxy cement. The tubes delimited an area of 3.46 cm^2 and were filled with the testing solution, 0.05 M NaCl. A three-electrode arrangement was used with a saturated calomel reference electrode, a platinum counter electrode and the exposed sample area as working electrode. The cell was connected to an Autolab PGstat 302N (Eco Chemie, The Netherlands) and all measurements were performed at room temperature with the cells inside a Faraday cage. Impedance measurements were done in the 100 kHz to 5 mHz frequency range with 7 points per decade distributed logarithmically; the sinusoidal perturbation was 10 mV rms at open circuit potential (OCP).

2.5. Surface analysis

A Hitachi S-4100 Scanning Electron Microscope was used to study the surface morphology.

3. Results

3.1. SEM

Fig. 1 depicts surface and cross-sectional microscopic views of the commercial weldable primer (WP1). The zinc particles are well visible and covered by a thin layer of polymer. The pictures reveal the shape, size and distribution of the zinc particles along the surface and show that most of them are not in contact with other particles. Micrographs of WP1 after 15 days of immersion in 0.05 M NaCl are presented in Fig. 2. These primers corrode in a localized manner with the formation of small blisters, as will be described later. Fig. 2(a) shows the less corroded region of the sample and Fig. 2(b) shows a cross-section detail of the border of a blister. In Fig. 2(a) corrosion is observed mainly in the zinc particles. There is no continuous film of corrosion products and the image suggests that most particles corrode isolated from the others. The inset shows the corrosion products covering the top of the particles, which is the area most accessible to solution. A thick layer of corrosion products is deposited on the top of the paint film close to the blisters, Fig. 2(b). This figure indicates that blisters come associated with the undermining of the zinc layer that dissolves completely exposing the steel base underneath. The undermining of the zinc layer extends about 100 µm away from the blister limit. The description for corroded WP1 applies also to WP2–WP4. WP5 showed a smaller degree of attack and only traces of corrosion products were found on particles of WP6.

3.2. SVET

Pictures and SVET maps of the bare substrate (EG) and all weldable primers obtained after 1 h, 1 day and 7 days of immersion in 0.05 M NaCl are shown in Fig. 3. After 1 h of immersion, SVET detected intense corrosion activity on the bare substrate and it was already possible to detected corrosion activity in the commercial WP as well as in the modified formulations WP2–WP4. Local anodes (in red, positive currents) were surrounded by a larger cathodic area with smaller current density (in blue, negative currents). No activity was detected on samples WP5 and WP6. After 1 day of immersion, the EG sample presented round shaped pits on the zinc coating. The SVET map showed anodic activity coincident with the pits and the remaining area was cathodic. Corrosion spots (blisters) were observed, by the naked eye, in WP1–WP3, most of them coincident with the anodic spots measured by SVET in the first hours. A small spot was also detected in WP4. No signs of degradation were detected in the samples with 55AlZn particles, WP5 and WP6. After 7 days of immersion, the EG presented severe attack with nearly half of the area without zinc layer. The SVET map showed small

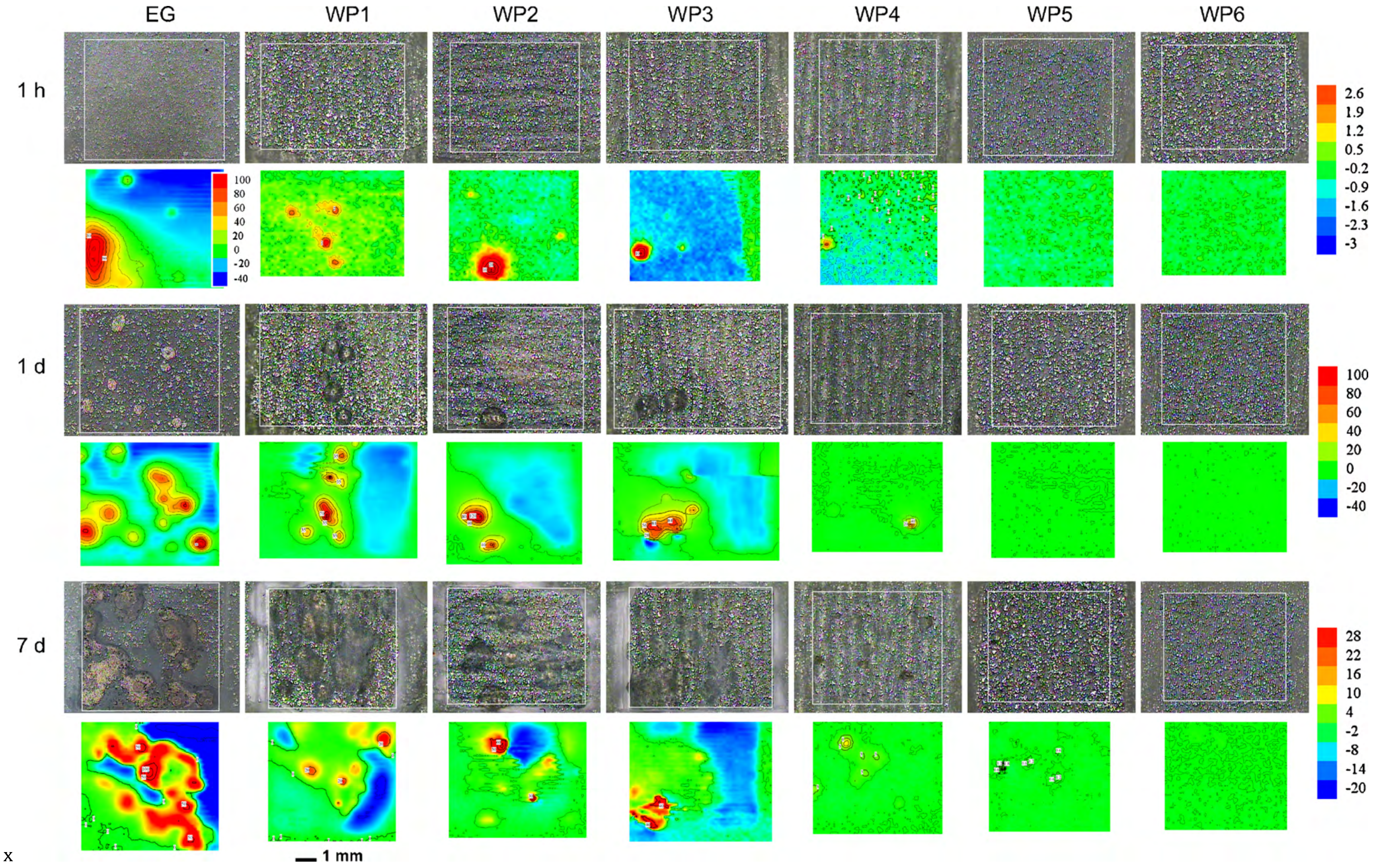

Fig. 3. Sample images and SVET maps of the uncoated metallic substrate and the WPs after 1 h, 1 day and 7 days of immersion in 0.05 M NaCl. Current scales are in μA cm^{-2}. The white rectangles show the position of the maps over the samples.

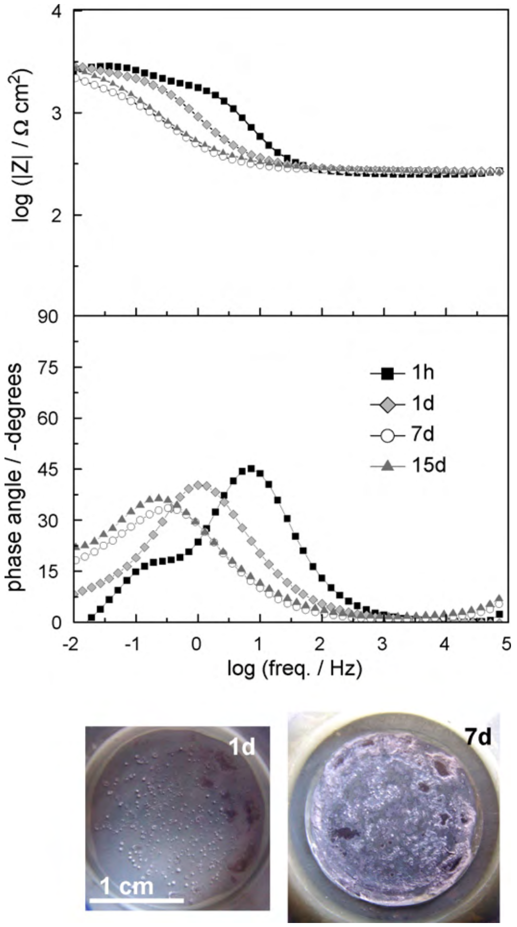

Fig. 4. Impedance response of the metallic substrate, EG, and samples' aspect after 1 day and 7 days of immersion. The sample area is 3.46 cm^2.

currents on the exposed steel area, strong anodic currents in the zinc layer close to the exposed steel and strong cathodic currents in the remaining zinc layer. Primers WP1–WP3 presented strong attack in both pictures and maps. WP4 also showed clear evidences of attack. Small signs of corrosion were detected in WP5 while WP6 was the only system that remained undamaged.

The corrosion pattern observed with EG has been previously described [6,7]. WPs seem to follow the same degradation pattern but the thin coating layer retards the corrosion rate, as supported by optical imaging and SVET currents on bare and coated samples. The rate varies with the protective quality of the primer, faster in WP1–WP3, slower in WP5 and WP6.

The signals measured by SVET came from the corrosion of the metal substrate and not from the corrosion of the zinc particles. The zinc powder particles are too small (~11 μm) and only a few of them have direct contact with other zinc particles in the paint. They are unable to generate currents strong enough to be detected 200 μm above in the solution. Experimentally, this was confirmed by dispersing zinc powder in the bottom of a Petri dish and filling it with 0.05 M NaCl, so that only single particles or small agglomerates existed. No activity was detected by SVET even though the optical pictures showed zinc corrosion products covering the particles and agglomerates. The results are given in the Supplementary Material.

3.3. EIS

Fig. 4 shows a Bode plot of the impedance response of EG. It is essential to know the behaviour of the uncoated metallic substrate to better recognize the protective effects of the coating systems applied on the top of it. The impedance of EG is small, starting from a few kΩ cm^2 at the beginning of immersion and rapidly dropping to values around 1 kΩ cm^2. Two time constants are observed. The one at high frequencies changes placement, from 10 Hz at 1 h to 0.5 Hz after 7 days of immersion. The surface of the sample becomes covered by a white deposit of corrosion products and the steel base is exposed in several regions.

Bode plots of the impedance response of WPs are presented in Fig. 5. The impedance of primers WP1 to WP4 has a fast drop from $\sim 10^5\ \Omega\,cm^2$ after 1 h of immersion to values close to the bare substrate after a few hours of immersion. The drop in WP5 is not so abrupt ($10^{6.3}$ to $10^5\ \Omega\,cm^2$ during the first day) and WP6 is the system with the highest impedance (10^7 to $10^6\ \Omega\,cm^2$ in the first day). The response of primers WP1–WP4 exhibits two time constants after just 1 h of immersion, while WP5 shows only one after 24 h and WP6 shows a second time constant only after 7 days. The time constant at higher frequencies ($\sim 10^4$–10^5 Hz) in WP1–WP4 changes rapidly during the first hours of immersion and after 1 day it has been replaced by another time constant at medium frequencies (10–10^3 Hz). After 1 day of immersion the impedance of samples WP1–WP4 is close to the impedance of the bare substrate and small blisters are observed on their surfaces. The blisters grow in number and size with time of immersion. At 15 days (end of the testing), after removing solution and drying, the surfaces show deposits of white corrosion products, abundant in WP1–WP4, small in WP5 and absent (by the naked eye) in WP6. To better understand the EIS results, a set of experiments was performed. In one experiment, the impedance of system WP1 was monitored during the first 3 h of immersion with fast scans. The results are depicted in Fig. 6(a) where it is clearly visible a single time constant response turning into a two time constant response in less than 1 h of immersion. In the light of what is commonly accepted for the degradation of painted metals [8,9], the first time constant, at higher frequencies, is associated to the response of the paint film with a film capacitance (C_f) and a film (or pore) resistance (R_f). The second time constant is usually associated to the corrosion of the metal substrate when it becomes in contact with the solution. A double layer capacitance (C_{dl}) and a charge transfer resistance (R_{ct}) are measured under these conditions. Fig. 6(a) depicts a fast increase in C_f and decrease in R_f (see the Supplementary Material for these values). This is interpreted as a result of rapid water absorption and, due to the small film thickness, film saturation and water accumulation at the metal-paint interface. In another experiment – Fig. 6(b) – small defects were produced in the paint film down to the substrate in a way that the exposed area increased by steps. This induced a rapid separation of the responses from the paint film and from the processes occurring at the metal surface, evident in the phase angle plot. In this experiment, and for the short time of testing, the values of C_f remained in the range of nF cm^{-2}, which is typical for an organic coating, while R_f decreased with the area of the defects (the values are given in the Supplementary Material). A possible time constant at low frequencies (<1 Hz) was not considered in the analysis of Fig. 6(a) and (b). These two experiments prove that the time constant measured at the higher frequencies of the spectrum corresponds to the response of the paint film and vanishes in a few hours of immersion for WP1.

A third experiment intended to correlate the two time constants that appear in WP1–WP4 after 1 day of immersion with the active and passive circuit elements in the corroding system. With that purpose, a WP1 sample after 1 day of immersion was subjected to small polarization tests. R_f and C_f are unaffected by small changes in dc

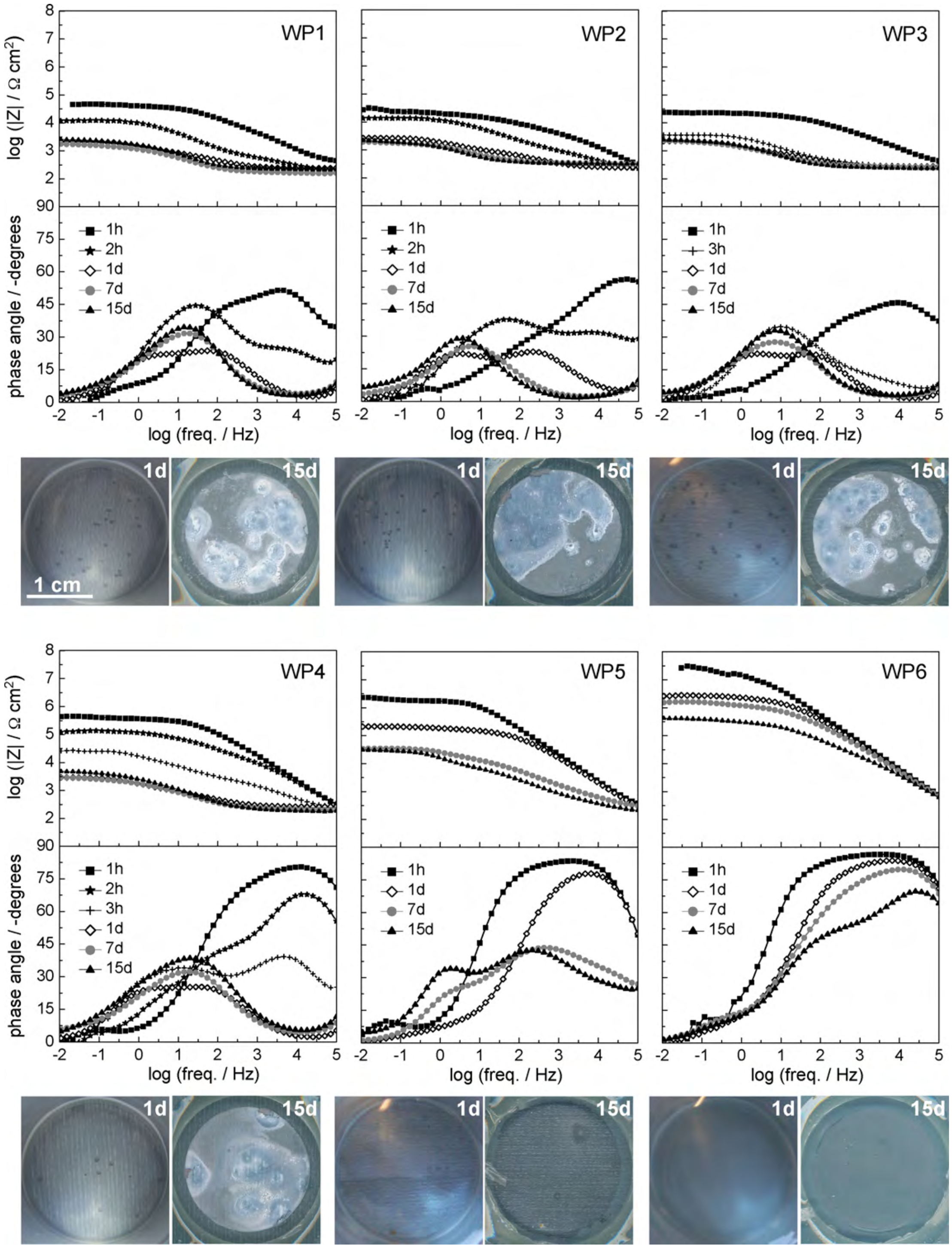

Fig. 5. Impedance response of the six weldable primers at different times of immersion in 0.05 M NaCl and samples' aspect after 1 day and 15 days of immersion. The sample area is 3.46 cm^2.

polarization. On the contrary, R_{ct} and C_{dl} vary with the dc potential applied during the EIS measurements. R_{ct}, for example, becomes smaller for potentials less negative than the corrosion potential (or OCP), since metal oxidation is favoured. Conversely, the application of potentials more negative than OCP tends to increase R_{ct}, indicating a slower and more difficult corrosion process. This can be seen in Fig. 6(c) with the responses of the sample at OCP and at ±20 mV *vs.* OCP. The response at 10–10^4 Hz is influenced by the small dc polarization and can be assigned to the corrosive processes occurring at the metal surface. The time constant at high frequencies remains unchanged. It is not the response of the paint film, as concluded from the two previous experiments. Its nature is not clear but it may be related with the accumulation of corrosion products on the top of the active metal areas (inside the blisters?), introducing an extra impedance to the flow of signal during the EIS measurement.

4. Discussion

Based on the experimental results, it is now possible to present a sequence of events for the degradation of weldable primers

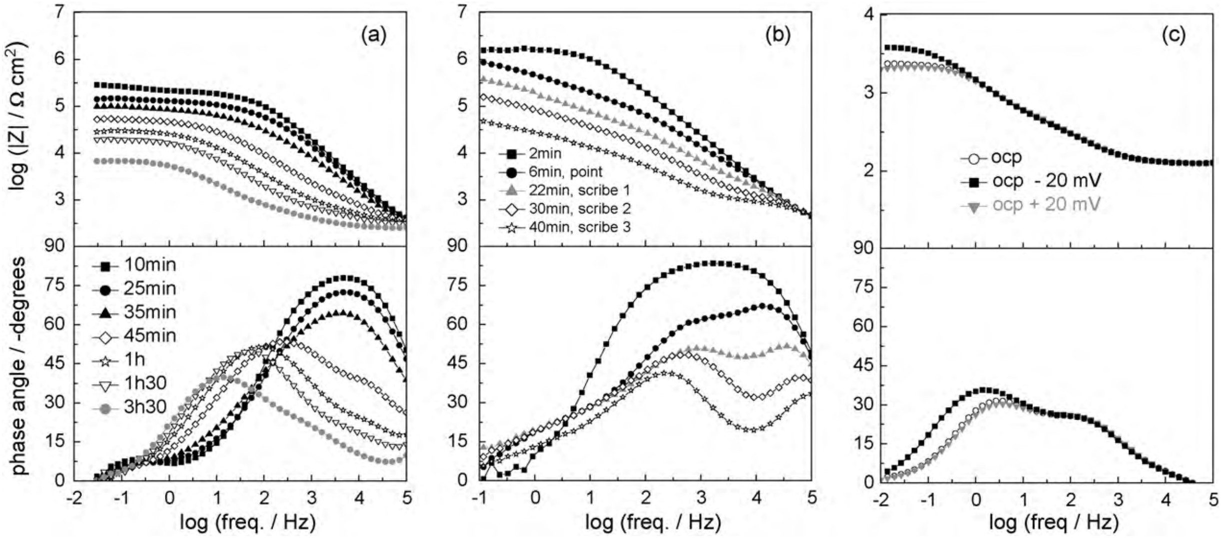

Fig. 6. Impedance response of the commercial primer (WP1): (a) during the first hours of immersion, (b) with artificial defects made in the first minutes of immersion and (c) with small anodic and cathodic polarizations after 1 day of immersion.

immersed in 0.05 M NaCl. The equivalent electric circuits in Fig. 7 will be used for that purpose. Numerical fitting of the impedance was made with the ZView2 software (Scribner Associates, USA) replacing the capacitors of the circuits by constant phase elements (CPEs). After fitting, the capacitances were calculated using the equation proposed by Hsu and Mansfeld [10]:

$$C = Y_0(\omega''_m)^{n-1}$$

where C is the capacitance, Y_0 is the frequency independent admittance of the CPE, ω''_m is the angular frequency at which the imaginary part of impedance is maximum and n is the CPE exponent. Fig. 8 shows the evolution of the fitted parameters with time of immersion.

As pointed out by visual observation and by SVET, the corrosion of the bare substrate, EG, takes place in a localized manner with round shaped anodes (pits) scattered through the surface. When the steel base becomes exposed it will be cathodically protected and zinc corrosion continues by enlargement of original pits and by appearance of new ones [6,7]. The metal-solution interface can be described by the electrical equivalent circuit presented in Fig. 7(a), where R_s is the solution resistance, C_{dl} and R_{ct} were presented above and Z_{dif} is the impedance of a mass transport process. Z_{dif} is responsible for the second time constant observed at lower frequencies in Fig. 4. When the metal substrate is coated by weldable primers, the impedance response is described by the circuit in Fig. 7(b) (the elements were already presented). At this stage, only the response due to the paint is detected. With time, water, ions and gases from the environment reach the metal surface and corrosion becomes possible. A circuit with two time constants, one for paint response and another for metal corrosion, is needed to explain the impedance response (Fig. 7(c)). Better protective paints take longer to transit from circuit (b) to (c). Primers WP1–WP4 took less than 1 h for this transition which reflects their poor barrier properties. After 1 day of immersion the paint film of these systems is no longer detected in the EIS measurements but the spectra still show two time constants. The response is fitted using the circuit of Fig. 7(d) where the new time constant is attributed to a contribution of corrosion products deposited on the top of active metal area (R_{ox} and C_{ox}). The corrosion of the zinc layer, in a localized manner down to steel, creates a separation between paint and metal substrate that leads to blister formation and growth. The coalescence of blisters produces extended areas of paint delamination. Later, probably with the increase of the active corroded area, the response becomes described by the equivalent circuit used for the bare substrate (Fig. 7(a)) but without the mass transport impedance. Degradation is slower for systems with 55AlZn particles and a three time constant response is observed in WP6 at 15 days of immersion. The circuit presented in Fig. 7(e) was used to fit the spectra of WP5 and WP6 obtained after 7 days of immersion and accounts for the contributions of paint film, oxide layer (native and/or from corrosion products) and corrosion process. While other circuits could have been used, this is the simplest one that fits the experimental data and complies with the physical description of the corroding system.

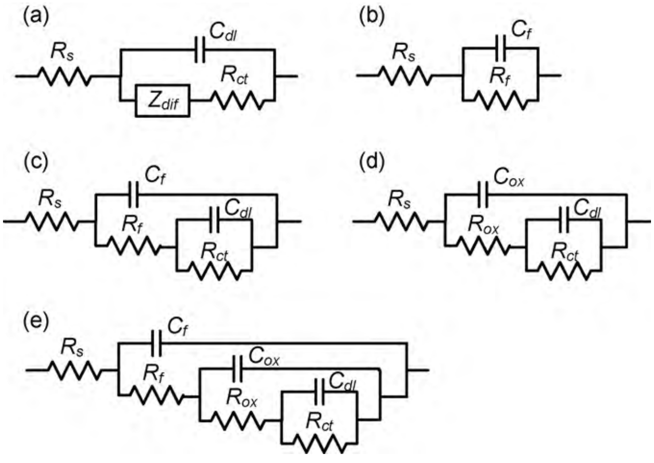

Fig. 7. Equivalent electric circuits used to fit the impedance response.

Fig. 8 shows that fitted values are similar for primers WP1–WP4. Parameters related with the paint response vanished in less than 1 day, R_{ct} values are in the same order of magnitude as those for EG and C_{dl} is smaller compared to the uncoated substrate. WP5 performs better than any other system with the same thickness, WP1–WP4. The best performance is achieved by the thicker 55AlZn system, WP6.

The metallic particles incorporated in the primer seem to play a critical role. WP5 is similar to WP1–WP4 except for the particles used (it has the same film thickness), but the corrosion rate is noticeably slower. It appears that the particle–binder interac-

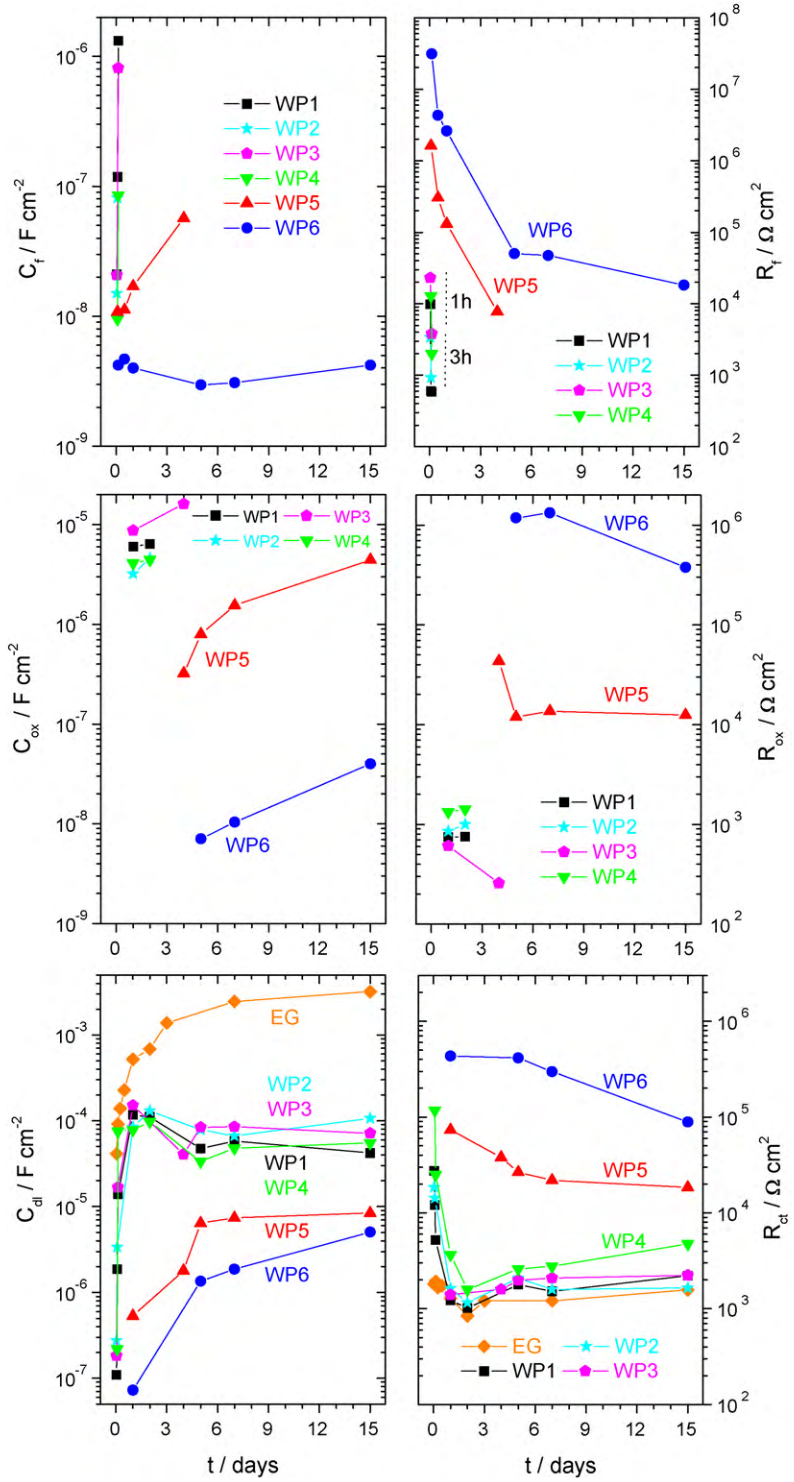

Fig. 8. Evolution with the time of immersion of R_f, C_f, R_{ox}, C_{ox}, R_{ct} and C_{dl}, determined by numerical fitting of the experimental EIS spectra.

tion is weaker with zinc powder and the particles' surface rapidly becomes wetted and oxidized. It is presumed that water reaches the metal substrate and ionic pathways are created through the entire surface mainly across the particles–matrix interface. This explains the rapid water uptake, low barrier properties and fast corrosion of the systems with zinc powder. The treatment of the zinc particles surface with corrosion inhibitors didn't bring any improvement. The organosilane led to a slight better performance in the SVET measurements. Being it an adhesion promoter the particle–binder bonding was probably strengthened. However, in the EIS measurements the performance was better than WP1–WP3 only in the very first hours of immersion. After 1 day the impedance response was already similar to WP1–WP4. The replacement of zinc powder by 55AlZn particles, on the other hand, led to good corrosion resistance. The 55AlZn alloy is known to have better anti-corrosive performance compared to pure zinc due to the presence of aluminium that renders passive the metallic surface [11,12]. It is speculated that the reduced corrosion of the 55AlZn particles preserves the integrity of the particles–matrix interface for longer retarding the ingress of water. This leads to a slower degradation process. The mechanism, however, is the same as found for primers incorporating zinc particles. The weldability of these new primers is still a matter to be investigated.

5. Conclusions

Formulations of weldable primers with modified zinc powder were tested in order to improve the corrosion resistance. The pre-treatment of zinc powder with corrosion inhibitors (cerium nitrate and 2-mercaptobenzothiazole) or with an organosilane (3-glycidoxypropyltrimethoxysilane) had no significant effect. On the other hand, the replacement of zinc powder by powder of 55AlZn gave a better corrosion resistance compared to the commercial system used by the automotive industry. For this system, two thicknesses were tested: 3.5 and 6.5 μm. Superior anticorrosive performance is obtained when thicker paints are used. For the moment this is not viable since good weldability needs thin films.

Acknowledgements

The authors acknowledge financial support from the Research Fund for Coal and Steel, contract no. RFS-CR-04031. A. C. Bastos thanks Fundação para a Ciência e a Tecnologia (Portugal) for a post-doctoral grant.

Appendix A. Supplementary data

Supplementary data associated with this article can be found, in the online version, at doi:10.1016/j.porgcoat.2010.04.021.

References

[1] A. Schnell, F. Androsch, K. Stellnberger, Revue de Métallurgie 7–8 (2004) 537.
[2] A. Besseyrias, C. Magny, Galvatech 2004 Conference Proceedings, 2004, p. 271.
[3] A.C. Bastos, S.V. Lamaka, M.L. Zheludkevich, M.G.S. Ferreira, Mater. Sci. Forum 587–588 (2008) 1003–1007.
[4] A.C. Bastos, M.L. Zheludkevich, M.G.S. Ferreira, Prog. Org. Coat. 63 (2008) 282–290.
[5] EN 10130:1991+A1:1998. Cold rolled low carbon steel flat products for cold forming. Technical delivery conditions.
[6] A.C. Bastos, A.M. Simões, M.G.S. Ferreira, Port. Electrochim. Acta 21 (2003) 371.
[7] A.C. Bastos, A.M.P. Simões, Prog. Org. Coat 65 (2009) 295.
[8] G.W. Walter, Corros. Sci. 26 (1986) 681.
[9] A. Amirudin, D. Thierry, Prog. Org. Coat. 26 (1995) 1.
[10] C.H. Hsu, F. Mansfeld, Corrosion (NACE) 57 (2001) 747.
[11] A.R. Marder, Prog. Mater. Sci. 45 (2000) 191.
[12] W.-B. Chen, P. Chen, H.Y. Chen, J. Wu, W.-T. Tsai, Appl. Surf. Sci. 187 (2002) 154.